Non-invasive Iridium Oxide Biopotential Electrodes

N. S. Dias*, A. F. Silva, P. M. Mendes, J. H. Correia
Dept. of Industrial Electronics, Campus Azurem, University of Minho, 4800-058 Guimaraes
*ndias@dei.uminho.pt

***Abstract*- Biopotential recording electrodes have been used to monitor non-invasively electroencephalogram (EEG), electromyogram (EMG) and electrocardiogram (ECG) by means of electrolyte pastes that improve electrode-skin interface. However, the skin preparation of 32 EEG electrodes may take up to 45 min. Despite the low skin-contact impedance and reasonable stability of the standard Ag/AgCl electrodes, several authors have been suggesting iridium oxide (IrO) as a promising biopotential recording and stimulation material. Hence, IrO thin-films were reactively DC-sputtered onto silicon substrates and electrochemically compared to the Ag/AgCl recording electrodes. The IS results observed for the IrO coatings were comparable to the results observed for the standard Ag/AgCl electrodes. The present work introduces a new IrO electrode with microtip structures that penetrate the outer skin layer (i.e. *stratum corneum*) that is 10 µm thick. The tip structures (100-200 µm high) were micromachined through a wet etching process with undercut in a KOH solution. The proposed dry electrode needs no paste application for signal quality improvement since it is in direct contact with the electrolytic fluids of the inner skin layers. A physiological experiment suggests that the IrO electrodes with microtips perform equally to the standard Ag/AgCl biopotential electrodes. The new dry IrO electrode is suggested to reduce the preparation period before the biopotential acquisition and for surface stimulation of excitable tissues.**

I. INTRODUCTION

Recent advances in the biomedical field related with medicine and biology have been demanding more sophisticated electrode fabrication technologies [1]. Electrical activity occurs between neurons as well as in the muscles (e.g. heart) and nerves. The biopotential electrodes, jointly with acquisition systems, sense the electrical activity and make it accessible for clinical and research trials. Electrodes may also be employed on stimulation of excitable tissue.

Biopotential recording and excitable tissue stimulation have been accomplished by recurring to invasive and non-invasive electrodes. The neuroscience field has been demanding invasive electrodes that are implanted for single and multiple recording sites, deep brain stimulation (DBS) and alleviate symptoms of Parkinson's disease [2]. Non-invasive electrodes are used for biopotential recordings like ElectroEncephaloGram (EEG) [3], ElectroOculoGram (EOG), ElectroCardioGram (ECG), ElectroMyoGram (EMG), among several other signals from the skin surface. The surface functional electrical stimulation (FES) [4] and electrotactile stimulation [5] is also accomplished by non-invasive electrodes.

It has been stated that skin impedance is determined mainly by the *stratum corneum* at frequencies below 10 KHz [6]. This outer skin layer has high-impedance characteristics since it is mainly constituted by dead skin cells and has very small water content [6]. Consequently, standard biopotential recording electrodes require skin preparation (e.g. skin abrasion) and use of electrolytic gel to bypass the *stratum corneum* isolation properties (Figure 1a). The preparation time for 32 standard EEG electrodes may take up to 45 min. Therefore, biopotential electrodes with microtips that are able to penetrate the outer skin layer and interface to the electrolytic fluids (abundance of some chlorides like NaCl) of living epidermis are of great interest (Figure 1b).

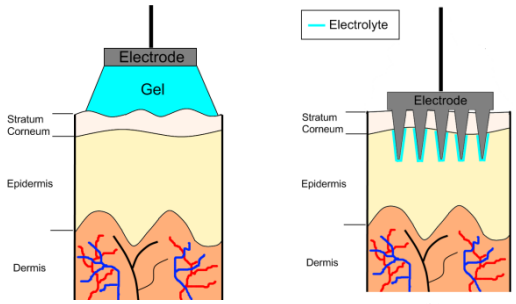

(a) (b)

Figure 1. Application of biopotential electrodes: (a) standard EEG electrode; (b) EEG electrode with microtips.

Different electrode materials have been tested on biopotential recording systems: Ag/AgCl [7], TiN [8], Al [9], Platinum [10] and Iridium oxide (IrO) [11]. Standard sintered Ag/AgCl electrodes are frequently used for clinical and biomedical applications (e.g. EEG and ECG) and they usually present very low skin-contact impedances and reasonable stability over the required frequency range (1-1000 Hz). Ag/AgCl has also been proposed as an electrode coating for dry electrodes with microtips [12]. However, the silver chloride showed to be toxic and has an associated infection risk since it dissolves on skin [8, 13]. IrO has been proved to be one of the most promising materials for tissue stimulation (due to its high charge delivery capacity, low constant impedance over the entire frequency range for neural stimulation and biocompatibility) [14-16] and for biopotential recording [17].

Initially in this work, DC-sputtered IrO thin-film electrodes are compared to the standard Ag/AgCl electrodes during Electrode-Electrolyte Impedance Spectroscopy (IS) analyses. The fabrication process of a new electrode with

micromachined tips is presented. The fabricated tips are about 100-200 μm high (Figure 2) in order to be able to pass through the outer skin layer (i.e. *stratum corneum*). IrO thin-films are DC-sputtered onto the microtips electrode. A performance comparison between the microtips electrode with IrO coating and the standard Ag/AgCl electrodes takes place during an EOG experiment.

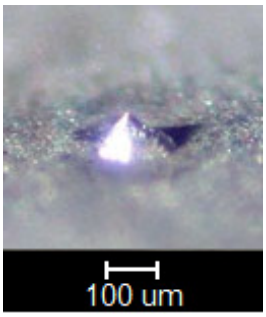

Figure 2. Optical microscope image of a microtip structure with pyramidal shape.

II. COMPARISON BETWEEN IRIDIUM OXIDE AND SILVER CHLORIDE ELECTRODES

Sputtering Sessions of Iridium Oxide Electrodes

IrO enables the use of the microelectrode as a mean of recording biopotentials and also as a way for functional electro-stimulation [15]. The low resistance of the pure iridium ensures good capabilities for recording purposes and the possibility of sputtering an oxide ensures the path to generate a redox reaction needed for the electro-stimulation.

Among other deposition processes, reactive sputtering of IrO enables high quality thin-film deposition in terms of homogeneity, at reduced costs. The IrO target are either DC-powered [18] or RF-powered [14] in a plasma environment. A sputtering deposition system was used for deposition of IrO thin-films onto silicon wafers. The characterization of the IrO thin-films is detailed on subsection II.A.

A *TRUMPF FPG 1500 DC* generator was employed for plasma application in a reactively sputtered environment with Ar/O_2 plasmas after a titanium (Ti) adhesion layer deposition on the substrates. The film thickness was determined by an optic-mechanical process executed with a *CSM Instrument Calotest*. The sputtering chamber was evacuated to 10^{-6} mbar by a cryogenic pump before every deposition. A throttle valve controlled the pumping speed, keeping a 55% conductance.

Different sputtering session were done, all performed at the same Argon working gas flow (75 sccm) and DC-power (700 W), but at different oxygen flow rates. As Figure 3 depicts, the increase of oxygen flow changes the surface to a more grainy and fractal surface, where seems to be starting a loss of coherence and mechanical stability.

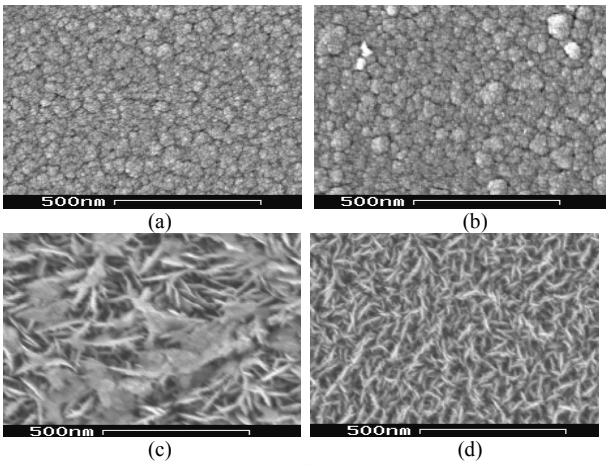

Figure 3. SEM images of IrO thin-film surfaces deposited at different oxygen flows: (a) 2 sccm; (b) 3.5 sccm; (c) 6.5 sccm; (d) 10 sccm.

An oxygen flow of 3.5 sccm seems to be a transition point between stable and unstable thin-film structures and was preferred as the electrode coating for the electrodes under evaluation. The deposition parameters are summarized in Table 1. IrO was also sputtered onto silicon wafers with the micromachined tips to be introduced on section III.

The film resistance is a crucial issue for biopotential recording electrodes. The resistance of the film was measured through the *van der Pauw* method [19] and its lowest value along all the sputtering sessions was $166.4E^{-07}$ ohm×cm in a 2 μm thick film.

TABLE 1. SPUTTERING PARAMETERS

		Sput. #1	**Sput. #2**
Target	**-**	**Ti**	**Ir**
DC Power	**W**	250	700
Argon flow	**sccm**	55	75
Oxygen flow	**sccm**	-	3.5
Throttle	**%**	15	55
Temperature	**ºC**	RT.	200
Duration	**min**	18	60

A. Electrode Characterization

Impedance Spectroscopy (IS)

A standard electrolytic experiment was employed in order to assess the electrochemical characteristics of both the sputtered IrO and Ag/AgCl electrodes as well as their interface with the electrolyte. An aqueous NaCl solution (most important fluid in the human tissue) with the concentration of 0.9% by weight was used as the electrolyte solution. The Na^+ and Cl^- ions are charge carriers free to migrate in an electric field, thus contributing to DC conductivity [6]. An electrode pair of each type was submersed in the electrolyte solution of the electrochemical cell at controlled inter-electrode distances.

In order to estimate the Electrode-Electrolyte Impedance (EEI) values, impedance spectroscopy measurements of the

electrode-electrolyte-electrode system were collected for the fabricated electrodes.

Although there are several other approaches for bio-impedance spectral evaluation [20], the one employed makes use of the digital signal generation capability of a regular PC equipped with Analogue-to-Digital Converter (ADC) and Digital-to-Analogue Converter (DAC) boards. A composite waveform, with a finite number of sinusoidal components, was used as the input signal (V_{in}) on the impedance to voltage converter circuit (Figure 4). Two PC equipped with Data Acquisition (DAQ) boards were used to implement the IS measurement system. The DAQ boards (National Instruments PCI6024E) used to stimulate the conversion circuit and measure its output are controlled by applications developed in Labview 7. One PC runs the waveform generation application to deliver the input signal (V_{in}) and the other one runs the data acquisition application to record the output signal (V_{out}). Accordingly, signal generation and signal recording were carried out by two distinct DAQ boards due to sampling rate limitations experienced for simultaneous signal generation and recording. The impedance conversion circuit has implemented a mechanism to limit the current (through $R_{current}$) that passes through the electrochemical cell (i.e. electrode-electrolyte-electrode sample). The current values that flowed through the solution were kept below 100 µA. $R_{current}$ value was 1 KΩ and the DC value of V_{out} was below 100 mV. The circuit on Figure 4 permits impedance measurements using only 2 electrodes since the operational amplifier 741 provides a virtual ground on its negative input.

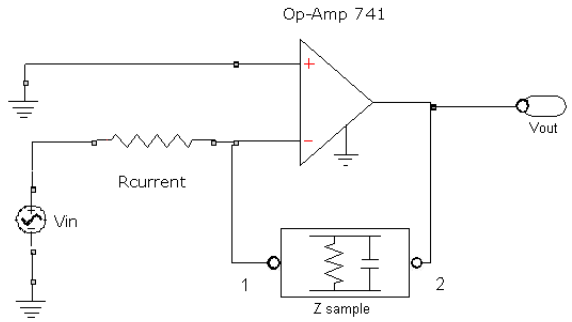

Figure 4. Impedance-voltage converter circuit based on the operational amplifier inverter configuration.

Characterization Results

On Figures 5 and 6, the conductivity and relative permittivity were plotted respectively for the whole frequency range 1-1000 Hz. The sample standard deviation is represented by a vertical bar for each measured frequency. In electrochemical analyses, the admittance values are often assessed instead of the impedance values actually read. It should be noted that the admittance ($Y=G+iB$, G is conductance, B is susceptance) is the reverse of the impedance values (impedance $Z=R+iX$, R is resistance, X is reactance). The conductivity is the cell-geometry-independent value of the conductance (G) and usually assumed as the reverse of the resistivity (i.e. material resistance that is independent of the cell-geometry). The conductivity ranges from around 5 mS/cm for 1 Hz to almost 14 mS/cm for 1000 Hz. The IrO electrodes show a conductivity that is significantly different from the AgCl electrode for frequencies below 3 Hz. The electrodes exhibit comparable conductivity for frequencies above 3 Hz. Relative permittivity (ε_r) is the cell-geometry-independent value of the susceptance (B) in respect to vacuum permittivity (ε_0 is $8.8e10^{-14}$ F/cm) and gives some insight about the amount of capacitive behavior of each electrode type. The AgCl electrodes relative permittivity ranges from 3.5×10^5 for 1000 Hz to 10^{10} for 1 Hz. The IrO electrodes present slightly higher relative permittivity than AgCl electrodes for frequencies below 3 Hz.

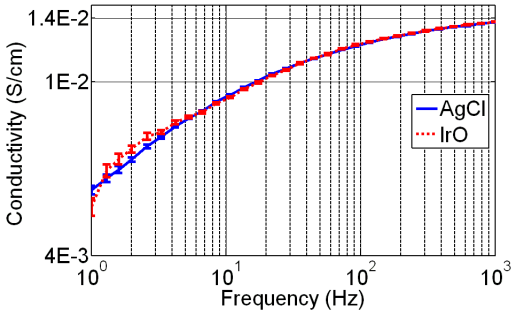

Figure 5. Conductivity (σ) of the fabricated electrodes (red dashed line) and of the control Ag/AgCl electrodes (blue solid line), for the whole frequency range (1-1000 Hz).

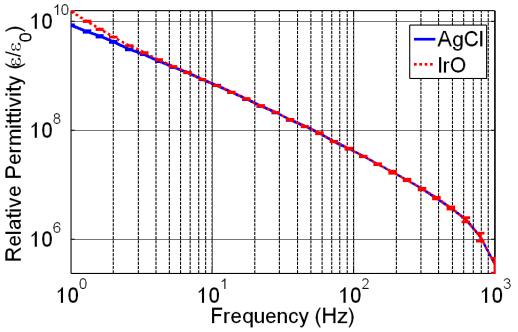

Figure 6. Relative permittivity (ε_R) of the fabricated IrO2 electrodes (red dashed line) and of the control Ag/AgCl electrodes (blue solid line), for the whole frequency range (1-1000 Hz).

Figure 7 represents the impedance phase measured for both electrodes. The AgCl electrodes presented an impedance phase of -40º for 1 Hz that decreases with frequency until it gets around 0º for 1 KHz. The IrO electrodes manifested significantly higher impedance phase values (-67º for 1 Hz) for frequencies below 3 Hz. The higher permittivity exhibited by IrO electrodes for frequencies below 3 Hz, in addition to a more negative impedance phase, suggest that the IrO electrodes are more capacitive than AgCl electrodes for low frequencies. For frequencies above 3 Hz, both electrodes show comparable behaviour in conductivity, permittivity and phase plots. Both electrodes show comparable performance over the entire frequency range.

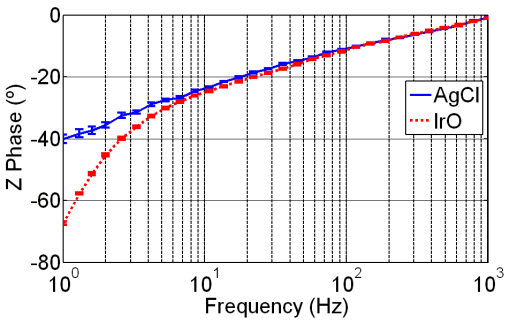

Figure 7. Impedance phase measured for the fabricated IrO2 electrodes (red dashed line) and the control Ag/AgCl electrodes (blue solid line) for the whole frequency range (1-1000 Hz).

III. MICROTIPS ELECTRODE

Electrode microtips fabrication

A wet-etch process using KOH was applied in the microfabrication of the silicon microtips. The tip shape was defined by the undercut effect in the etch process, where locally fastest-etching planes are revealed.

A standard silicon wafer with 500 µm width and [100] orientation was used with two silicon nitride (SiN) layers (top and bottom) as masks for the etching. The microfabrication process of the microtips is illustrated in Figure 8.

In the first step (Figure 8a), a mask with 200 µm square features was used on the lithography process for microtip definition. The chosen size for the mask features came as a result of previous analysis of the mask characteristics effect. The 200 µm offered not only a locked aspect ratio in terms of print resolution, but also provided better control of the etching progression, since more time was needed for the tip formation.

In the second step (Figure 8b), the photoresist was removed from the areas that were not covered by the photomask. Then, the opened windows in the SiN layer allowed exposition to its elimination in the third step (Figure 8c). In the next two steps (Figures 8d and 8e), the photoresist was removed and the Si wafer was etched. The remaining areas with SiN worked out as a protection layer for the etching process of the Si wafer with a 30% KOH solution at a temperature of 87°C, ensuring a etch rate of 1.6 µm/min. In the last step (Figure 8f), the SiN remaining on the electrode surface was removed by hydrofluoric acid (HF).

The microtips emerged from the undercut effect on the etch process, which was documented by means of optical microscopy every 30 minutes. Figure 9 presents the evolution of the etching process from which is possible to follow the progress of the lateral plans that form a three dimensional structure. The etching process employed is anisotropic, with an angle of 54.7º in the [111] plane. The higher etching rate of the top plan, when compared to the side plan etching rate, was responsible for the pyramidal structure in Figure 2. Due to the anisotropic process, the square corners were etched and the final structure has hexagonal shape.

Figure 10 illustrates an electrode array with 4×4 microtips.

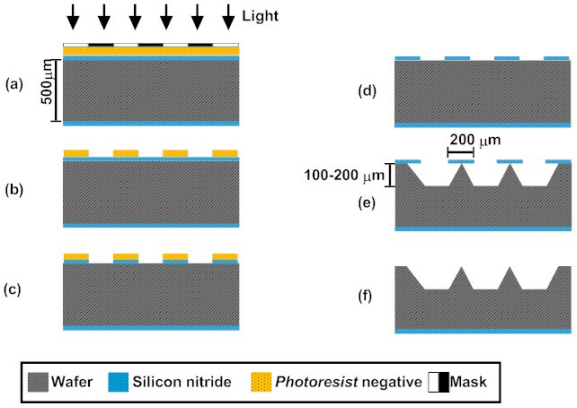

Figure 8. Schematic of the 6 steps employed on the microtip structures fabrication.

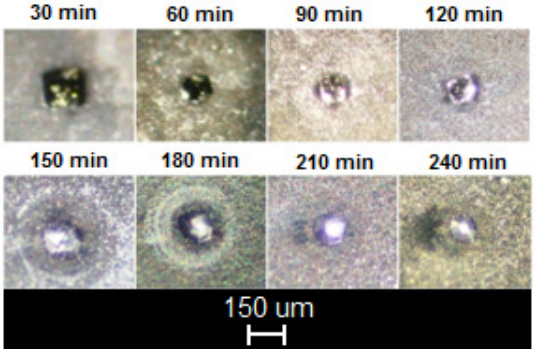

Figure 9. Top view of etching progression stages with 30 min intervals.

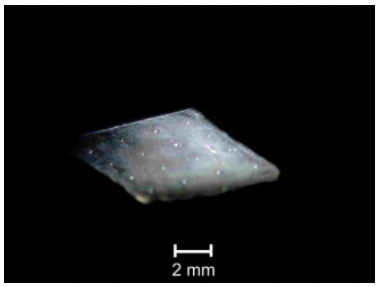

Figure 10. Optic microscope image of a microtips array.

ElectroOculoGram (EOG) Experiment

A preliminary performance evaluation of the microtips electrode with IrO coating took place during an EOG experiment. The EOG was recorded by means of electrodes laterally placed at the *canthi* of the eyes. As a result of the cornoretinal standing voltage potential (the cornea is positive relative to the retinal *fundus*), the eye movements produce changes in the potential between electrodes.

The microtips array and the standard commercially available Ag/AgCl electrodes were placed horizontally to the eyes (horizontal EOG) and both signals were recorded simultaneously. Ag/AgCl electrodes were placed after a previous skin preparation (i.e. skin abrasion) and standard electrolytic gel was used to improve electrode-skin interface. Neither skin preparation nor electrolytic gel was applied to the electrodes with microtips.

EOG data were acquired at 2000 samples/s by an EEG acquisition system with 22 bits resolution. The signals of both electrode types were digitally band-filtered (1-40 Hz) and a notch filter was also applied (50 Hz) to avoid the major interference of the electrical mains. Butherworth (zero-phase corrected) filters were employed.

The subject was instructed to sequentially look to one of two points that were horizontally equidistant from the centre of his visual field. The subject performed three eye movement trials of 1 min each, with 1 min long inter-trial period (i.e. resting period). The whole EOG session took 5 minutes.

Figure 11 presents 3 s of the recorded EOG data for both the Ag/AgCl electrode and the microtips electrode. The EOG data, with around 1 mV amplitude (peak-to-peak), were recorded when the subject was instructed to make eye horizontal movements. Although the Ag/AgCl electrode was applied after a previous skin preparation and the microtips electrode directly applied on skin, both electrodes present similar signals.

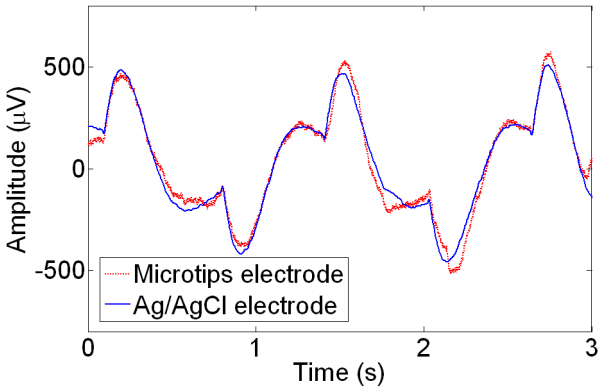

Figure 11. Time-domain recorded signals from both the control Ag/AgCl electrodes (blue solid line) and the microtips electrode with IrO coating (red dashed line) during an EOG experiment.

IV. Discussion and Conclusions

This study introduced a new IrO electrode with microtips for biopotential recordings. The new dry electrodes are intended to avoid skin preparation (i.e. electrolyte application and skin abrasion).

The conductivity values suggested that the resistive behaviours of both recording materials (Ag/AgCl and IrO) are comparable for the whole frequency range. The conductivity increases steadily until the 1 KHz frequency limit suggesting that there is no leakage currents through the substrate for the frequency range of interest.

The unequal behaviour of the IrO and Ag/AgCl materials, for frequencies below 3 Hz, seems due to different kind of charge transmissions. The chemical reactions that assure the electron and ion exchange between non-polarizable electrodes and the electrolyte seem to occur with more extent at the Ag/AgCl electrodes than at the IrO electrodes, for low frequencies. This is in agreement with the general knowledge that IrO coatings tend to produce polarizable electrodes (interface can be modelled by a capacitance) and Ag/AgCl are non-polarizable electrodes. Figures 6 and 7 illustrate the capacitive behaviour of the IrO electrodes: IrO electrodes present higher permittivity (capacitance is directly proportional to permittivity) than Ag/AgCl electrodes for low frequencies; impedance phase is more negative for IrO than for Ag/AgCl electrodes at low-frequencies. It should be noted that the electron exchange reactions are an undesired phenomenon at minimally-invasive dry electrodes that are supposed to pass through the outer skin layer. Tissue damage due to excessive accumulation of ions such as Cl^- (infection risk) or even electrode degradation is more likely in these conditions. Hence, DC currents should be avoided and polarizable electrodes must be employed. In those cases, AC currents are measured through the electrical double layer that is formed at the electrode-electrolyte interface. The double layer capacitance values are dependent on the type of metal, the surface conditions, the type of electrolyte and the applied voltage. Despite the quality of the signals collected by the microtips array during the EOG experiment, the electrode-tissue interface can still be improved by increasing their surface permeability and making the surface to be dendrite structured [14]. These techniques increase the surface area of the electrode that is in contact with the electrolyte. As far as the surface area enlargement does not compromise the electrode mechanical stability, it seems to be a reliable way to decrease the electrode-tissue impedance and improve signal-to-noise ratio.

The signals recorded during the EOG experiment for both the standard Ag/AgCl and the microtip electrodes show acceptable signal-to-noise ratio and look very similar for the horizontal eye movement task employed. These results suggest that the microtips array with IrO coating may resemble the traditional Ag/AgCl electrodes for acquisition of biosignals whose DC component can be filtered out.

From previous studies about stimulating materials, iridium oxide showed to over perform Ag/AgCl in respect to charge delivery capacity and low-constant transition impedance [15]. IrO also demonstrated long-term mechanical stability and corrosion resistance. Therefore, considering the comparable performance of both materials for recording purposes suggested by the presented results, IrO is proposed to coat a microtip structured biopotential electrode array with recording and stimulation capabilities. The 100-200 μm high microtips and the high charge delivery capacity of IrO make this electrode suitable for electrotactile stimulation applications. The ability to bypass the outer skin layer (10 μm thick) brings the electrode near the excitable nerves which decreases the potential value needed for tactile sensor stimulation. Assistive technologies for motor impaired people like Brain-Computer Interfaces (BCIs) benefit of alternative feedback pathways to close the control loop whenever the other sensory inputs (e.g. sight, hearing) are impaired or disturbed [21].

A dry electrode that can be used simultaneously for biopotential recording (e.g. EEG, EOG, EMG) and

electrotactile stimulation (e.g. mouth, forehead or arms stimulation) permit a new generation of human-machine interaction in non-restrained environments (i.e. subject senses, like sight or hearing, are exposed to random and unpredictable stimuli). A three-dimensional structure (microtip) capable of bypassing the skin non-conductive layer, with a low resistance IrO film on its surface, permits the construction of a biopotential recording/stimulating electrode with fast application.

Future work will focus on the improvement of the microtip aspect ratio and the fixation of the electrodes in the skin.

ACKNOWLEDGMENT

N. S. Dias is supported by Portuguese Foundation for Science and Technology (SFRH/BD/21529/2005). A. F. Silva is supported by Portuguese Foundation for Science and Technology (SFRH/BD/39459/2007).

REFERENCES

[1] W. R. Patterson et al., "A Microelectrode/Microelectronic Hybrid Device for Brain Implantable Neuroprosthesis Applications," *IEEE Transactions on Biomedical Engineering*, vol. 51, no. 10, October 2004.

[2] A. Lebedev and M. A. L. Nicolelis, "Brain–machine interfaces: past, present and future," *TRENDS in Neurosciences*, vol. 29, no. 9, pp. 536-546, July 2006.

[3] P. Griss et al., "Micromachined Electrodes for Biopotential Measurements," *Journal of Microelectromechanical Systems*, vol. 10, no. 1, pp. 10-16, March 2001.

[4] V. K. Mushahwar, P. L. Jacobs, R. A. Normann, R. J. Triolo, and N. Kleitman, "New functional electrical stimulation approaches to standing and walking," *J. Neural Eng.*, vol. 4, pp. 181-197, 2007.

[5] J. Webster, P. Bach-y-Rita and W. Tompkins K. Kaczmarek, "Electrotactile and vibrotactile displays for sensory substitution systems," *IEEE Transactions on Biomedical Engineering*, vol. 38, pp. 1-16, 1991.

[6] S. Grimnes and Ø. G. Martinsen, *Bioimpedance anb bioelectricity basics*. London, UK: Academic Press, 2000.

[7] J. A. McLaughlin, E. T. McAdams, and J. M. Anderson, "Novel dry electrode ECG sensor system," in *Annual Int. Conf. EMBC*, 1994, p. 16.

[8] W. M. Heuvelman, P. Helderman, G. C. A. M. Janssen, and S. Radelaar, "TiN reactive sputter deposition studied as a function of the pumping speed," *Thin Solid Films*, vol. 332, pp. 335-339, 1998.

[9] A. Lopez and P. C. Richardson, "Capacitive electrocardiographic and bioelectric electrodes," *IEEE Transactions on Biomedical Engineering*, vol. 16, p. 99, 1969.

[10] A. Ivorra et al., "Minimally invasive silicon probe for electrical impedance measurements in small animals," *Biosensors & Bioelectronics*, vol. 19, pp. 391-399, 2003.

[11] T. D. Plante, and J. Ehrlich S. F. Cogan, "Sputtered iridium oxide films (SIROFs) for low-impedance neural stimulation and recording electrodes," in *Proceedings of the 26th Annual International Conference of the IEEE EMBS*, San Francisco, CA, USA, 2004, pp. 4153-4156.

[12] P. Griss, H. K. Tolvanen-Laakso, P. Meriläinen, and G. Stemme, "Characterization of Micromachined Spiked Biopotential Electrodes," *IEEE Transactions on Biomedical Engineering*, vol. 49, no. 6, pp. 597-604, June 2002.

[13] T. C. Ferree, P. Luu, G. S. Russell, and D. M. Tucker, "Scalp electrode impedance, infection risk, and EEG data quality," *Clinical Neurophysiology*, vol. 112, pp. 536-544, 2001.

[14] Wessling, W. Mokwa, and U. Schnakenberg, "RF Sputtering of iridium oxide to be used as stimulation material in functional medical implants," *Journal of Micromechanical and Microengineering*, vol. 16, pp. 142-148, 2006.

[15] E. Slavcheva, R. Vitushinsky, Mokwa W., and U. Schnakenberg, "Sputtered iridium oxide films as charge injection material for functional electrostimulation," *Journal of Electrochemical Society*, vol. 151, pp. 226-237, 2004.

[16] W. Mokwa, "MEMS technologies for epiretinal stimulation of the retina," *Journal of Micromechanics and Microengineering*, vol. 14, pp. 12-16, 2004.

[17] R. D. Meyer, S. F. Cogan, T. H. Nguyen, and R. D. Rauh, "Electrodeposited Iridium Oxide for Neural Stimulation and Recording Electrodes," *IEEE Transactions on Neural Systems and Rehabilitation Engineering*, vol. 9, no. 1, pp. 2-11, March 2001.

[18] A. Belkind et al., "Characterization of pulsed dc magnetron sputtering plasmas," *New J. of Physics*, vol. 7, pp. 1-16, 2005.

[19] L.J. van der Pauw, "A method of measuring the resistivity and Hall coefficient on lamellae of arbitrary shape," *Philips Technical Review*, vol. 20, pp. 220-224, 1958.

[20] J. D. Bronzino, *The biomedical engineering handbook vol. II*, J. D. Bronzino, Ed. Connecticut, U.S.A.: Taylor & Francis CRC, 2006.

[21] A. Chatterjee, V. Aggarwal, A. Ramos, S. Acharya, and N. V. Thakor, "A brain-computer interface with vibrotactile biofeedback for haptic information," *Journal of Neuroeng. and Rehab.*, vol. 4, pp. 40-52, 2007.